Bone morphogenetic protein 8A plays a role in the maintenance of spermatogenesis and the integrity of the epididymis

Guang-Quan Zhao[1,2], Lucy Liaw* and Brigid L. M. Hogan[1,†]

[1]Howard Hughes Medical Institute and Department of Cell Biology, Vanderbilt University Medical School, Nashville, TN 37232-2175, USA
[2]Department of Pathobiology, College of Veterinary Medicine, University of Missouri, Columbia, MO 65211-5300, USA
*Current address: Division of Cardiology, Department of Medicine, Nashville, TN 37232-6300, USA
[†]Address for correspondence (e-mail: brigid.hogan@mcmail.vanderbilt.edu)

SUMMARY

The murine *Bmp8a* and *Bmp8b* genes are tightly linked on mouse chromosome 4 and have similar expression during reproduction. Previous studies have shown that targeted mutagenesis of *Bmp8b* causes male infertility due to germ cell degeneration. To investigate the function of *Bmp8a*, we have inactivated the gene by homologous recombination. Heterozygous and homozygous *Bmp8a* mutants reveal normal embryonic and postnatal development. Despite high levels of *Bmp8a* expression in the deciduum, homozygous mutant females have normal fertility, suggesting that the gene is not essential for female reproduction. *Bmp8a* and *Bmp8b* are expressed in similar patterns in male germ cells. Unlike homozygous *Bmp8b^{tm1}*

mutants, homozygous *Bmp8a^{tm1}* males do not show obvious germ cell defects during the initiation of spermatogenesis. However, germ cell degeneration is observed in 47% of adult homozygous *Bmp8a^{tm1}* males, establishing a role of *Bmp8a* in the maintenance of spermatogenesis. A small proportion of the mating homozygous *Bmp8a^{tm1}* males also show degeneration of the epididymal epithelium, indicating a novel role for BMPs in the control of epididymal function.

Key words: *Bmp8a*, Targeted gene inactivation, Male germ cell, Spermatogenesis, Epididymis, Fertility, Mouse, Bone morphogenetic protein

INTRODUCTION

Bone morphogenetic proteins (BMPs) are intercellular signaling molecules with multiple functions during development and differentiation in both vertebrates and invertebrates (Gelbart et al., 1989; Hogan et al., 1994a; Hogan, 1996). They belong to the TGF-β superfamily of growth factors and bind as homodimers or heterodimers to heteromeric transmembrane serine/threonine kinase receptor complexes (Kingsley, 1994; Massagué et al., 1994; McPherron and Lee, 1996; Hogan, 1996). This ligand and receptor interaction triggers a downstream signaling cascade leading to a variety of biological responses, including changes in cell proliferation, survival, differentiation and cell fate.

BMP8A and BMP8B belong to the 60A subfamily, which includes the vertebrate BMP5, BMP6 and BMP7, and the *Drosophila* 60A proteins (Zhao and Hogan, 1996; Hogan, 1996). Mutations in several of these genes cause severe developmental abnormalities in different cell types and tissues. For example, mutations in the mouse *Bmp5* gene result in a short-ear phenotype with abnormalities in the development of certain cartilages and bones, as well as lung and urogenital defects in some genetic backgrounds (Kingsley et al., 1992). *Bmp7* homozygous mutant mice die shortly after birth due to

failure of kidney development accompanied by abnormal eye development and skeletal malformation (Dudley et al., 1995; Luo et al., 1995).

Murine *Bmp8a* and *Bmp8b* have similar genomic organization, are closely linked on mouse chromosome 4 (at least within 0.2 cM, data not shown), share high levels of sequence identity and have similar expression patterns in reproductive organs, suggesting that they arose through recent gene duplication (Zhao and Hogan, 1996). During pregnancy, *Bmp8a* (but not *Bmp8b*) is expressed at high levels in the decidual cells of the uterus, while *Bmp8b* (but not *Bmp8a*) is expressed at high levels in the trophoblasts of the placenta. Therefore, both genes may play a role during implantation and placental development. They are the first members of the *Bmp* family found to be expressed in male germ cells in a bimodal manner. Before 3.5 weeks of age, low levels of transcripts for both genes are found in a majority of spermatogonia and primary spermatocytes. Subsequently, however, the expression of both *Bmp8* genes shifts to stage 6-8 round spermatids where transcripts are detected at higher levels than in spermatogonia (Zhao and Hogan, 1996; Zhao et al., 1996).

To investigate the functions of *Bmp8* genes during reproduction, we have initiated a molecular genetic approach by introducing targeted mutations into each gene. In the absence of

a functional *Bmp8b* gene, male germ cell proliferation is significantly reduced during early puberty and there is also a marked increase in male germ cell apoptosis in the adult. Eventually, the majority of the *Bmp8b* homozygous mutant males show severe seminiferous tubule degeneration and become sterile. Therefore, *Bmp8b* is required for both the initiation and maintenance of spermatogenesis in the mouse (Zhao et al., 1996). To similarly investigate the function of *Bmp8a* during spermatogenesis and pregnancy, we have inactivated the mouse gene by homologous recombination in embryonic stem (ES) cells. Here, we report the phenotypic analysis of *Bmp8a* mutants and *Bmp8a/Bmp8b* compound heterozygous mice.

MATERIALS AND METHODS

Construction of the targeting vector

Bmp8a genomic DNA clones were isolated as described previously (Zhao et al., 1996). Two overlapping genomic clones covering exons 2-7 were mapped by restriction enzyme digestion as shown in Fig. 1A. A replacement vector was constructed using 1.2 kb 5′ and 4.5 kb (5′ portion of the second phage clone) 3′ homology arms as indicated. As described previously (Zhao et al., 1996), PGK-TKA+ (Rudnicki

et al., 1992) and MC1DT-A (Yagi et al., 1990) cassettes were attached to the 5′ and 3′ ends of the vector for negative selection. In the targeted allele, exons 4-6 are replaced with a PGK-neo^r cassette (Rudnicki et al., 1992). This *Bmp8a* mutant allele is designated *Bmp8a^{tm1blh}* according to standard nomenclature (Davisson 1995).

Generation of recombinant ES cell clones and mouse chimeras

TL1 ES cells of passage 11 and 12 were electroporated with 20-50 µg of the linearized targeting vector as described (Zhao et al., 1996). ES cell culture and drug selection were performed essentially as described (Winnier et al., 1995; Zhao et al., 1996). Three out of one hundred drug-resistant ES clones (A5, H4 and H9) contained a correctly recombined *Bmp8a^{tm1}* allele. All three lines were injected into C57BL/6 blastocysts to generate chimeras (Hogan et al., 1994b). *Bmp8a^{tm1}* was transmitted from A5 and H4 cells by mating male chimeras with Black Swiss females (Taconic Farm). Agouti animals were genotyped by Southern blotting.

Southern blot analysis for genotyping *Bmp8a* mutants

Genomic DNA was digested with *Eco*RI, size fractionated on a 0.8 % agarose gel, transferred to positively charged Nylon membrane and hybridized with two different probes. (1) A 5′ external *Bmp8a* cDNA probe, containing exons 2 and 3, hybridized to 9.0 kb and 8.0 kb bands from the wild-type *Bmp8a* and *Bmp8b* alleles, respectively, and to a
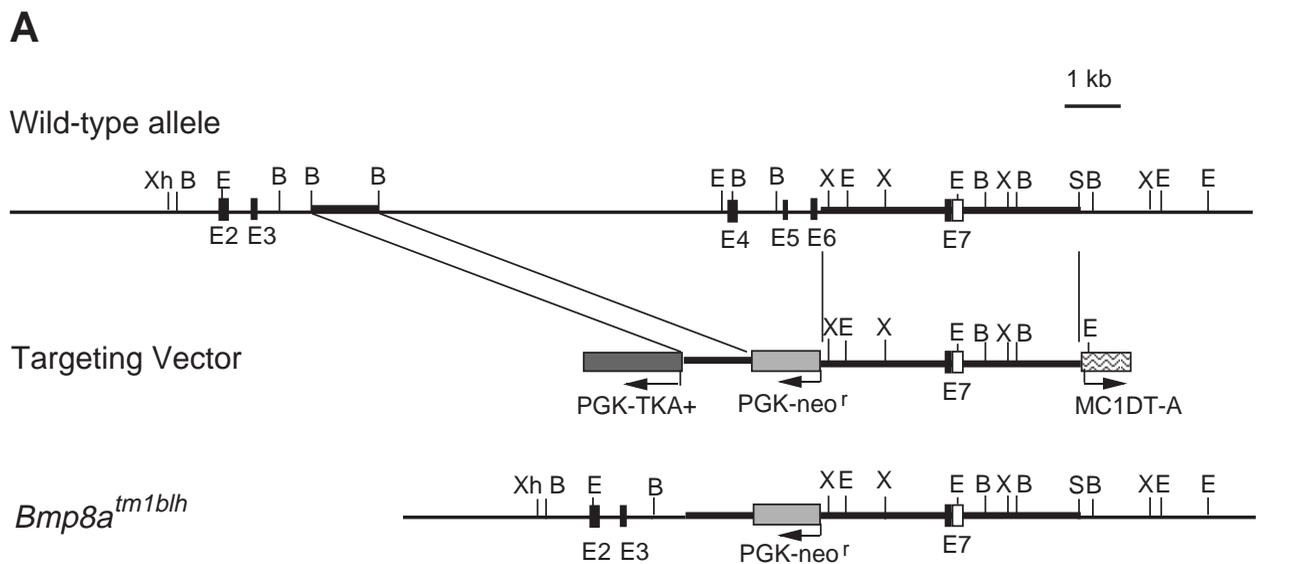

Fig. 1. Targeted mutagenesis of the mouse *Bmp8a* locus. (A) Schematic representation of the *Bmp8a* wild-type allele on the top, targeting construct in the middle and the recombinant *Bmp8a^{tm1blh}* allele at the bottom. Genomic DNA fragments used as the short (5′) and long (3′) homology arms of the targeting vector are indicated as thick solid lines. Coding exons 2, 3, 4, 5, 6 and the first half of exon 7 are indicated as solid boxes (E2-E7). The second half of exon 7 containing the 3′ untranslated region is indicated as an open box. Expression cassettes PGK-TKA+, PGK-neo^r and MC1DT-A are also shown as boxes with arrows indicating direction of transcription. Restriction enzyme abbreviations: (B) *Bam*HI; (E) *Eco*RI; (S) *Sal*I; (X) *Xba*I; (Xh) *Xho*I. (B) Genomic Southern blot with a cDNA probe derived from exons 2 and 3 of *Bmp8a*, which is almost identical in sequence to exons 2 and 3 of *Bmp8b*. Therefore, *Eco*RI-digested DNA reveals a 9 kb fragment for the wild-type *Bmp8a* locus and an 8 kb fragment for the wild-type *Bmp8b* locus. The 9 kb *Bmp8a* allele is reduced to 5 kb in the *Bmp8a^{tm1blh}* allele. (C) Genomic Southern blot using a cDNA fragment containing exons 4, 5, 6 and 7 as a probe. This probe is specific for *Bmp8a* and reveals two *Eco*RI fragments of 2.3 kb (containing exons 4, 5 and 6) and 2.0 kb (containing part of exon 7) for the wild-type allele and only a 2.0 kb fragment for the mutant allele.
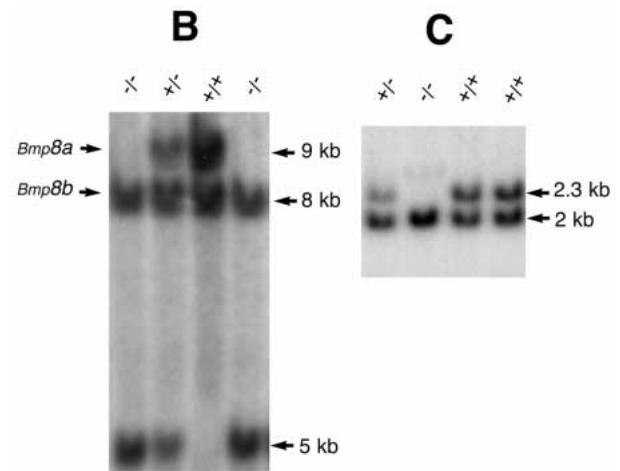
5.0 kb band from the *Bmp8a^(tm1)* allele (Fig. 1B). (2) A 3′ internal cDNA probe, containing exons 4, 5, 6 and 7, hybridized with 2.0 kb and 2.3 kb bands for the wild-type *Bmp8a* allele and only a 2.0 kb band for the *Bmp8a^(tm1)* allele (Fig. 1C).

Histology, TUNEL and in situ hybridization

For histology, freshly dissected testes were weighed and fixed in Bouin's fixative for 2-24 hours depending on the size. Mounted sections of 7 μm were stained either by hematoxylin/eosin or periodic acid-Schiff's reagent (PAS)/hematoxylin. Histological analysis of *Bmp8b* mutants (Zhao et al., 1996) and the initial survey of *Bmp8a* mutants in this study established that the testes from a single animal, when comparable in weight, usually have a similar histology. Therefore, one testis of each mouse was processed for histological analysis. Testes of different genotypes were embedded and sectioned in the same paraffin block and stained on the same slides. Histology was surveyed by microscopic examination of every third pair of sections; when abnormalities were found, adjacent sections were processed for further analysis. Seminiferous tubules with obviously compromised spermiogenesis were considered abnormal. A seminiferous tubule was also scored as a degenerating tubule if it contained more than 50 germ cells with condensed nuclei and eosinophilic cytoplasm in 10 consecutive sections (for characteristics of apoptosis see Zhao et al., 1996; Furuchi et al., 1996; Dix et al., 1996; Gavrieli et al., 1992). Of the testes examined, 47% (15/32) of the *Bmp8a* homozygous, 17% (3/18) of the *Bmp8a* heterozygous mutants and none (0/11) of the wild-type animals showed different degrees of germ cell degeneration.

TUNEL (terminal deoxynucleotide transferase-mediated dUTP nick end labeling) and in situ hybridization were performed essentially as described (Zhao et al., 1996; Zhao and Hogan, 1997).

Comparison of *Bmp8a* and *Bmp8b* expression levels

A reverse transcription-polymerase chain reaction (RT-PCR) approach was designed to compare the levels of *Bmp8* expression during spermatogenesis. RNA samples were isolated from testes of ICR mice at several stages (1, 2, 4, 6, 8 and 10 weeks of age) using the Ultraspec-II RNA isolation system (Biotecx, Houston). First-strand cDNA was prepared in 30 μl reaction volume using 5 units of AMV reverse transcriptase, 50 ng oligo d(T)$_{10}$ as primers and 5 μg of total RNA from each sample as template. The RT reaction was incubated at 42°C for 30 minutes and then 470 μl of H_2O was added to dilute the first-strand cDNA templates for PCR. Control DNA templates were prepared in the same way as RT reaction without AMV reverse transcriptase.

A region of *Bmp8* cDNAs across exons 2, 3 and 4 was selected for PCR amplification (nucleotides 417-829 of *Bmp8a*). More than 98% of the nucleotides in this region are identical between these genes. The oligonucleotide primers Bmp8-5′ com (GTG GAA CGC GAC CGT ACC CTG) and Bmp8-3′ com (ACC ATG AAA GGC TGT CTG GAG) were designed to match both genes. The final PCR volume was 50 μl containing 1 μl of the reverse transcription reaction products, 100 ng of each primer, 5 μl of 2.5 mM dNTP cocktails, 1.25 units of Taq DNA polymerase and 5 μl Buffer F of the PCR Optimizer (In Vitrogen). The PCR amplification profile was: 94°C 30 seconds, 63°C 30 seconds and 72°C 30 seconds. After 40 cycles, 10 μl of the PCR products were visible under ultraviolet light following agarose gel electrophoresis. However, no PCR products were observed when the PCR reaction was terminated at 35 cycles. Therefore, 30 cycles, before the PCR amplification had reached the plateau, was selected for subsequent amplification.

After amplification, the PCR products were precipitated together with 10 μg of bacterial tRNA as carrier and digested with 10 units of *Bam*HI for 5 hours in a final volume of 20 μl containing 2 μg pBluescript II KS plasmid DNA to monitor the efficiency of *Bam*HI digestion. The digested DNA was resolved on a 1.5% agarose gel for Southern hybridization using a 317 bp *Bmp8a* DNA probe (nucleotides 454-771). Hybridization was performed in Rapid-hyb

buffer (Amersham) at 60°C. The washed membrane was exposed to X-ray film for 3 hours. The 412 bp band corresponded to the intact *Bmp8b* DNA, while the 352 bp band corresponded to the *Bam*HI-digested *Bmp8a* DNA (Fig. 8B).

Electron microscopy (EM)

Mice were euthanized with CO_2 inhalation and cardiac perfusion was performed with 50 ml of 4% paraformaldehyde/0.1% glutaraldehyde phosphate buffer (pH 7.3). Testes were stored in the same fixative for 24 hours and washed 0.1% Cacodylate buffer (pH 7.35; 3× 5 minutes) and then minced into 1 mm cubes. After 2 rounds of 1% sucrose incubation at room temperature (30 minutes each), samples were postfixed in 2% osmium tetroxide/1% sucrose for 60 minutes at 4°C. The dehydrated samples were embedded in Epon. Semithin sections (1 μm) were processed and stained with toluidine blue for light microscopy, and seminiferous tubules with normal appearance were selected for thin sections and EM. Both *Bmp8a* mutant and wild-type testes were examined.

RESULTS

Targeted mutagenesis of the mouse *Bmp8a* gene

The mouse *Bmp8a* gene contains seven coding exons (Özkaynak et al., 1992). Exons 1, 2, 3 and the first half of exon 4 encode the signal peptide and the pro-region of the precursor protein, while the second half of exon 4, and exons 5, 6 and 7 encode the mature region. As shown in Fig. 1, in the *Bmp8a^(tm1)*
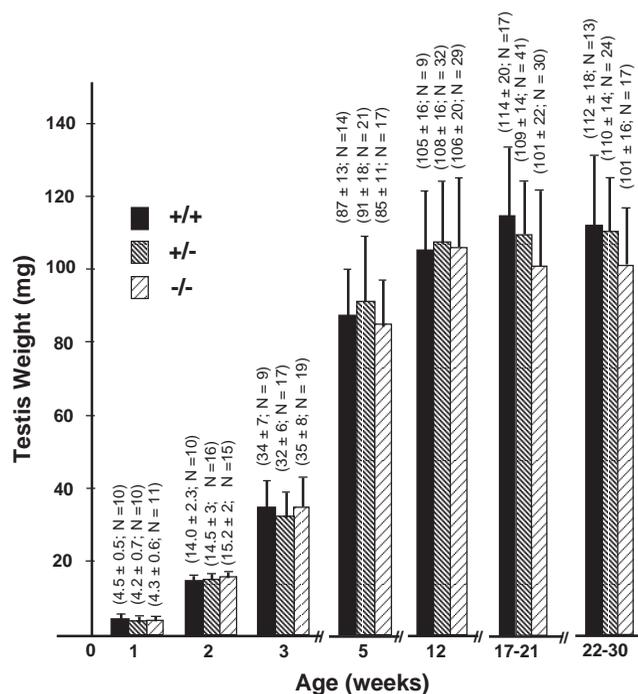

Fig. 2. Comparison of testis weight of wild-type (+/+) and *Bmp8a^(tm1blh)* mutant (+/− and −/−) mice. Testes from each age group were dissected out, blotted and weighed. Several litters were used for each group. Mean ± s.d. is indicated in brackets, N represents the total number of testes in each group. Generally, one testis from each animal was weighed if the sizes of both testes appeared comparable. If, in a very few cases, the size of the two testes appeared significantly different, both were weighed and the average was used for statistical analysis.

allele, an 8 kb genomic DNA fragment encompassing exons 4, 5 and 6 was replaced by a PGK-neo[r] cassette (Rudnicki et al., 1992) in the opposite transcriptional orientation. Therefore, DNA encoding part of the pro-region, the dibasic cleavage site RXXR and the majority of the mature region was removed. Furthermore, the remaining exons 3 and 7 are not in frame, should alternative splicing around the PGK-neo[r] cassette occur. It is predicted that no functional or dominant negative forms of BMP8A protein is made from the $Bmp8a^{tm1}$ allele, although in situ hybridization with ^{35}S-labeled riboprobes against the specific 3′ untranslated region of $Bmp8a$, detects a transcript in stage 6-8 round spermatids of homozygous mutant testes (data not shown).

After drug selection, three recombinant ES cell lines A5, H4 and H9 were obtained and injected into C57BL/6 blastocysts to generate chimeras. The $Bmp8a^{tm1}$ allele was transmitted to offspring in lines A5 and H4. Mutant mice from both ES cell lines exhibit similar phenotypes when maintained on a mixed genetic background of [129 × Black Swiss] for this study. All data reported here were generated from a combination of these two lines.

Reproductive performance of *Bmp8a* mutants

$Bmp8a$ expression was detected in the deciduum during pregnancy, in spermatogonia and primary spermatocytes during the initiation of spermatogenesis, and in stage 6-8 round spermatids during the maintenance of spermatogenesis (Zhao and Hogan, 1996; Zhao et al., 1996). This expression pattern raised the possibility that, without a functional $Bmp8a$ gene, both male and female reproduction would be compromised. During initial mating tests of heterozygous mutants, the expected ratio of wild-type (n=45), heterozygous (n=104) and homozygous mutant (n=52) offspring was obtained. The homozygous mutants grew normally to adulthood and appeared healthy. Therefore, $Bmp8a$ was not required for
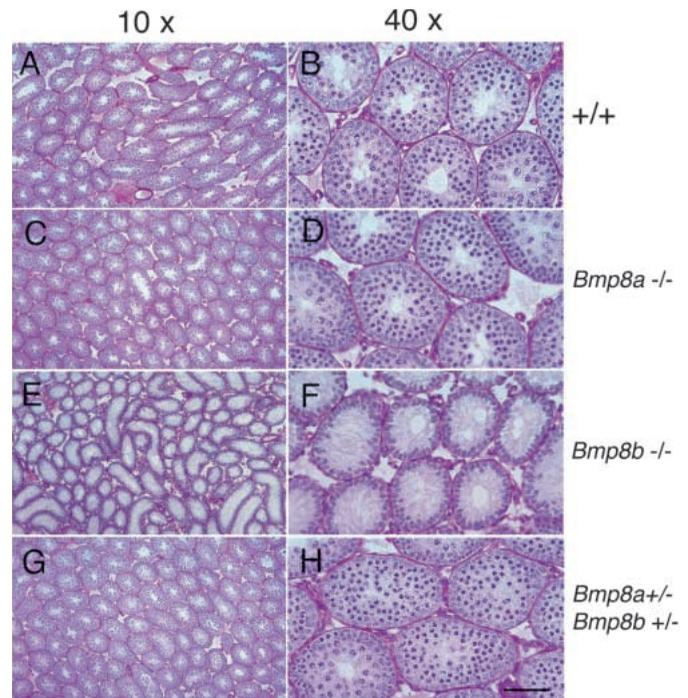

Fig. 3. Histological comparison of testes from 2 week-old animals of wild-type (+/+), *Bmp8a* −/−, *Bmp8b* −/− and *Bmp8* compound heterozygotes. (A,C,E,G) Low (×10) and (B,D,F,H) high (×40)-power photomicrographs, respectively. A typical representative histology from each genotype is shown. At this age, the testes of *Bmp8b* homozygous mutants are significantly smaller than the others and, in severe cases, only one layer of epithelium is present in the seminiferous tubule (E,F). In contrast, in wild-type, *Bmp8a* homozygous mutant and compound heterozygous mutant testes, multiple layers of germ cells are present in the seminiferous tubules. Bar = 200 μm (A,C,E,G); 50 μm (B,D,F,H).

Table 1. Mating test of *Bmp8atm1blh* mice

Male (n)	Female (n)	Litter number	Litter size (mean ± s.d)
+/+ (3) +/− (3)	−/− (18)	30	8.5±2.2
+/− (11)	+/− (23)	77	8.3±2.6
−/− (8)*	−/− (22)	85	8.1±2.6
−/− (8)†	+/− (20) +/+ (5)	66	8.3±2.8
Comp (6)‡	+/+ (10) Comp (10)	27	7.4±3.2

7- to 10-week-old mice of different genotypes were caged together for 9-20 weeks. Each male was housed with 2-4 females and pregnant females were separated before giving birth. Number of pups was recorded within 24 hours after birth. Most matings resulted in litters of normal frequency and size (wild-type mating gave an average litter size of 8-8.5 pups).

*One male in this group had two litters of 7-8 pups during the initial mating period, but was infertile thereafter, presumably due to epididymis degeneration and granuloma formation (Fig. 9B).

†One male in this group never reproduced and histology revealed severely compromised spermiogenesis.

‡Comp for Bmp8 compound heterozygotes. In this group, one male never reproduced and a cyst was found in the left testis. Another male had normal reproductive performance for 8-9 weeks, but did not reproduce for the last 6 weeks. Histological examination revealed epididymis degeneration and granuloma formation (Fig. 9C).

embryonic and postnatal development. We further tested the fertility of the homozygous $Bmp8a^{tm1}$ animals by mating with wild-type and heterozygous animals. As summarized in Table 1, all homozygous mutant females showed normal reproduction. All mutant males showed normal fertility initially. However, as they aged, some animals (2 out of 16) eventually became sterile. Therefore, $Bmp8a$ appears to play a role in the fertility of certain males, but not of females.

Bmp8a is not required for the initiation of spermatogenesis

As shown in Fig. 2, there is no significant difference in the average weights between testes of wild-type and $Bmp8a^{tm1}$ mutants. This is in contrast to our findings in $Bmp8b$ mutants, where testes of all homozygotes from 1 to 3 weeks of age are significantly smaller than those of wild-type (Zhao et al., 1996). Histological examination of more than 60 $Bmp8a$ homozygous mutants (at least 10 for each age group) revealed no abnormalities from 1 to 6 weeks of age. The exception to this was that one individual out of 30 examined at 2 weeks had a testis weight of 7 mg (12-15 mg for wild-type mice of the same age) with a histology similar to that of $Bmp8b$ mutants (Fig. 3E,F). This small testis and 14 more testes were not used for statistical analysis due to lacking litter mate wild-type and heterozygote controls.

Bmp8a plays a role in the maintenance of spermatogenesis

The testis weight of some *Bmp8a* mutants older than 17 weeks of age appears to be smaller than that of wild-type and heterozygotes (Fig. 2), although the difference is not statistically significant by Student's *t*-test (*P* is between 0.05 and 0.1). Histologically, about 47% of *Bmp8a* homozygous mutant testes (15 out of 32 testes) of 12- to 30-week-old males show varied degrees of germ cell degeneration (Figs 4, 5). As shown in Fig. 4C,D, the most severe germ cell deficiency observed in *Bmp8a* mutants (2 out of the 32 examined) is much milder than that in *Bmp8b* mutants (Fig. 4E,F). In many seminiferous tubules of such *Bmp8a* mutants, spermiogenesis is severely compromised, or even absent, while spermatogenesis (although abnormal) is still present. Increased meiotic germ cell apoptosis can be identified in numerous tubules (arrows in Fig. 4D). In the milder cases of germ cell deficiency, only a certain percentage of the seminiferous tubules (from one tubule to 50% of the tubules) of given sections show cellular degeneration, resulting in compromised spermiogenesis (Fig. 5D-O). The characteristics of the apoptotic germ cells are condensed and darkly stained nuclei or chromatin and strongly eosinophilic cytoplasm. As shown in Fig. 6, these cells can be labeled by TUNEL (Zhao et al., 1996; Furuchi et al., 1996; Dix et al., 1996; Gavrieli et al., 1992). Similar abnormalities are also observed in 17% of the *Bmp8a* heterozygous mutant testes (3 out of 18 examined) and half of the *Bmp8a/Bmp8b* compound heterozygotes (5 out of 11).

Electron microscopy (EM) of *Bmp8a* mutant testes was performed on seminiferous tubules with apparently normal spermatogenesis as revealed by initial light microscopy. When thin sections were examined under EM, most seminiferous tubules appeared to be similar to those in wild-type testes. However, a small percentage of the seminiferous tubules in some *Bmp8a* mutants contained increased number of apoptotic germ cells with darkly stained nuclei (Fig. 7). In these tubules, most pachytene spermatocytes showed normal morphology and synaptonemal complexes (SC) were found at a frequency comparable with those of wild-type mice. Therefore, the increased number of apoptotic pachytene spermatocytes in *Bmp8a* mutants is unlikely to be the result of a block in differentiation. Rather, it is likely to reflect decreased cell survival. The EM observations are consistent with our findings in *Bmp8b* mutants in which seminiferous tubules with normal spermatogenesis contained increased number of TUNEL-labeled spermatocytes (Zhao et al., 1996).

Bmp8a is expressed at lower levels than *Bmp8b* during the initiation of spermatogenesis

In situ hybridization showed that both *Bmp8* genes were expressed in a similar pattern in male germ cells (Zhao and Hogan, 1996; Zhao et al., 1996). However, *Bmp8a* mutants only displayed a mild germ cell degeneration during the maintenance of spermatogenesis. One explanation for this finding is that *Bmp8a* is expressed at lower levels than *Bmp8b* during spermatogenesis. To address this question, an experimental strategy combining RT-PCR, restriction enzyme digestion and Southern blotting was designed to compare the relative abundance of mRNAs for *Bmp8a* and *Bmp8b*.

As shown in Fig. 8A, the cDNAs encoding the pro-regions of BMP8A/B are highly conserved, allowing the co-amplification of these genes with a single pair of PCR primers. After amplification, the PCR products are digested with *Bam*HI, which cleaves the *Bmp8a* product at nucleotide 767, but not *Bmp8b*.
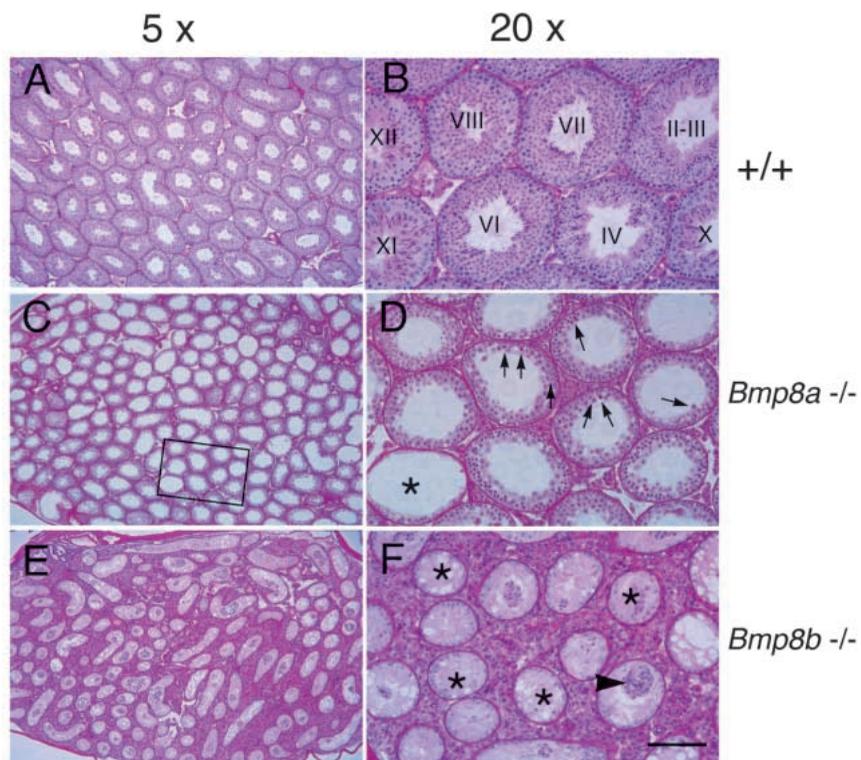

Fig. 4. Histological comparison of a wild-type and *Bmp8a* and *8b* homozygous mutant testes showing the most advanced germ cell degeneration observed. (A,C,E) Low (5×) and (B,D,F) high (20×)-power photomicrographs, respectively. (A,B) Sections of a wild-type testis (17 weeks of age) showing normal spermatogenesis in all seminiferous tubules (stages of each tubule are indicated by Roman Numerals; Russell et al., 1990). (C,D) Section of a homozygous *Bmp8a* mutant testis (22 weeks of age) with the most advanced germ cell degeneration observed. In this testis, very few spermatids were observed in the seminiferous tubules, while meiotic germ cells were found in most seminiferous tubules. However, a small number of tubules did lack most germ cells and even some of the Sertoli cells had disappeared (*). Apoptotic germ cells exhibiting darkly stained condensed nuclei were observed in most seminiferous tubules (arrows). (E,F) Sections of a homozygous *Bmp8b* mutant testis (22 weeks of age) showing that all seminiferous tubules lack spermatogenesis and only Sertoli cells were left in a majority of the seminiferous tubules (*). Some darkly stained cells (arrowhead) were observed in the center of some seminiferous tubules. These cells did not express Sertoli cell markers such *Dhh* and *Cp-2* (Zhao et al., 1996) and were most likely spermatogonia which had detached from the basal lamina. Bar = 400 μm (A,C,E); 100 μm (B,D,F).

Electrophoresis separates the *Bmp8a* and *Bmp8b* products, and Southern blotting hybridization with a common probe reflects the relative abundance of each message during spermatogenesis. As shown in Fig. 8B, at 1 week of age, the PCR products are predominantly from *Bmp8b*. As the mice age, *Bmp8a* expression levels increase, but at 2 and 4 weeks of age, *Bmp8b* PCR product is still more abundant than that of *Bmp8a*. However, after 6 weeks of age, the expression levels of *Bmp8a* and *Bmp8b* are comparable (data not shown for 6 and 8 weeks of age). The RT-PCR experiments were repeated three times with similar results.

Bmp8a plays a role in the maintenance of epididymis integrity

Most of the *Bmp8a* homozygous mutant males show normal reproduction (Table 1). However, one out of the 16 males tested was fertile within the first month of mating, but produced no offspring afterwards. This animal was killed at 4 months of age, revealing two adhesive clumps attached to the right epididymis – one attached to the caput, the other to the cauda. Histology revealed no obvious abnormality in the left testis and epididymis, but gross abnormalities of the right epididymis. As shown in Fig. 9B,E, a large granuloma-like mass, with sperm and some necrosis in the center and massive leukocyte infiltration on the periphery, almost replaced the cauda epididymis. Subsequently, similar but milder abnormalities were observed in another mating homozygous *Bmp8a* mutant and a *Bmp8a/Bmp8b* compound heterozygote (Fig. 9C,D,F,G). One interpretation of the phenotype was that the epithelium lining the epididymal tubules degenerated and sperm was forced out from the collapsed tubule. Due to the antigenicity of sperm, massive leukocyte infiltration would then accompany the eruption of the epididymal tubule, resulting in a granuloma-like mass. Similar degeneration of the epithelium and leukocyte infiltration was also found in the distal caput region of the same epididymides shown in Fig. 9B,C. However, in contrast to the mating group (2 out of 16 for *Bmp8a* homozygous mutants, 1 out of 6 for *Bmp8a/Bmp8b* compound heterozygous mutants), no granuloma-like pathology was found in the epididymides of more than 60 non-mating *Bmp8a* homozygous and *Bmp8* compound heterozygous males examined. Only epithelial degeneration was found in the distal caput region in 2 out of the 40 epididymides sectioned (Fig. 9H-J) and no obvious epididymal epithelium degeneration was found in the cauda region of the same epididymides.

Bmp8a and *Bmp7* are expressed in the initial segment of the caput epididymis

In light of the degeneration of the epididymal epithelium and granuloma formation in the *Bmp8a* mutants, we examined the expression of
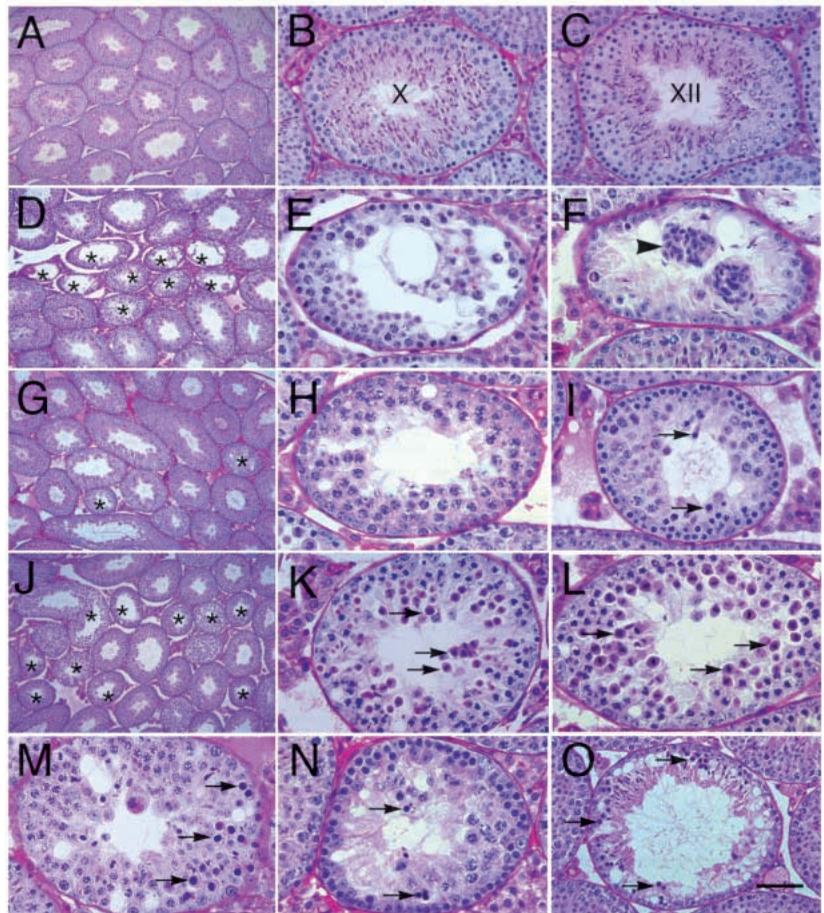

Fig. 5. Examples of milder forms of histological abnormalities in adult *Bmp8a* mutant testes. (A-C) Sections of a wild-type testis (22 weeks of age) showing normal spermatogenesis. (A) Low-power magnification; (B) A stage X seminiferous tubule at high-power magnification; (C) A stage XII seminiferous tubule at high-power magnification; (D-O) Representative sections from testes of different *Bmp8a* homozygous null mutants (12-30 weeks of age). (D) Low-power magnification showing numerous degenerating seminiferous tubules (*); (E,F) High-power photomicrographs of seminiferous tubules similar to those indicated in D. Only a few meiotic germ cells are present. Arrowhead indicates a cluster of darkly stained cells in the center of the degenerated tubule similar to those observed in *Bmp8b* mutant testis (Fig. 4F). (G) Low-power magnification showing germ cell degeneration in two seminiferous tubules (*). (H,I) Seminiferous tubules similar to those indicated in G. No spermatids are found in H and very few in I. A few apoptotic spermatocytes with condensed and darkly stained nuclei (small arrows) are present in I. (J) Low-power magnification showing germ cell degeneration in a large proportion of the seminiferous tubules (*). (K,L) Two examples showing that germ cells are blocked in metaphase and degenerating. They have darkly stained chromatin and eosinophilic cytoplasm (arrows). (M) A section of a seminiferous tubule containing 16 apparently apoptotic germ cells with condensed and darkly stained nuclei (arrows) in a small area of the tubule. Some of these cells are in close proximity to the basement membrane, suggesting that they are either dying spermatogonia or dying preleptotene spermatocytes. (N) A section of a seminiferous tubule in which no spermatids are present and most meiotic germ cells have disappeared. However, the spermatogonia and preleptotene spermatocyte populations seem to be relatively normal. Arrows indicate apoptotic cells. (O) A section of a seminiferous tubule showing most meiotic germ cells have degenerated. The remaining primary spermatocytes have condensed darkly stained nuclei (arrows). The presence of many elongated spermatids suggests that the previous round of meiosis was relatively unaffected. Bar = 200 μm (A,D,G,J); 50 μm (B,C,O); 30 μm (E,F,H,I,K,L,M,N).
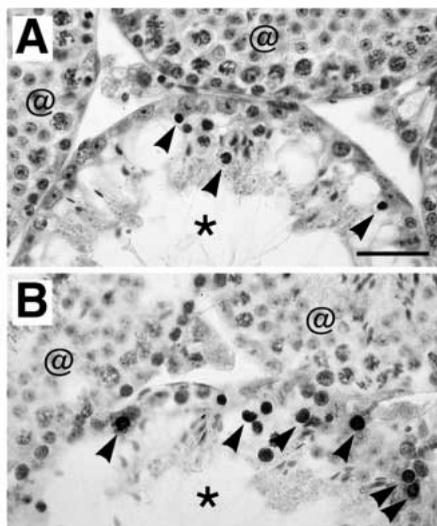
Fig. 6. TUNEL labeling of an adult *Bmp8a* mutant testis. (A) A section of a *Bmp8a* mutant testis (3 months of age) stained with PAS and hematoxylin, showing a degenerating seminiferous tubule (*) and two adjacent tubules with normal morphology (@). The darkly stained apoptotic germ cells are indicated by arrowheads. (B) A section 70 μm apart from A, showing numerous germ cells positively stained by TUNEL (arrowheads). Bar = 30 μm.

Bmp family members in the adult epididymides of mating and non-mating animals (14-17 weeks of age). Among the genes examined (*Bmp2, 4, 5, 6, 7, 8a, 8b* and *Vgr2*), only *Bmp8a* and *Bmp7* show unique expression in the initial segment. As shown in Fig. 10, both *Bmp8a* and *Bmp7* are expressed in the same region of the epididymis. However, the expression levels of *Bmp8a* in this region are lower than in the stage 6-8 round spermatids (Fig. 10A). Also, the levels of *Bmp7* expression in the initial segment are much higher than those of *Bmp8a*.

DISCUSSION

The role of *Bmp8a* in female reproduction

This paper and the previous study (Zhao et al., 1996) have shown that the absence of either *Bmp8* gene does not significantly affect female reproduction at a significant level. This may be due to compensation by other *Bmp*s transcribed in the deciduum and trophoblasts. For example, *Bmp4* is expressed in a similar pattern to that of *Bmp8b* in the placenta and *Bmp2* is expressed in a similar pattern to *Bmp8a* in the deciduum (data not shown). More sophisticated genetic approaches are required to address the functions of *Bmp*s during placenta development, such as creating compound mutations in *Bmp* genes, or tissue-specific inactivation of multiple genes encoding BMP ligands and receptors.

Bmp8a does not play a major role in the initiation of spermatogenesis

Both *Bmp8a* and *Bmp8b* transcripts were detected in spermatogonia and spermatocytes at low levels during the first wave of spermatogenesis (Zhao and Hogan,

1996; Zhao et al., 1996; Fig. 8). The targeted inactivation of *Bmp8b* results in a deficiency in male germ cell proliferation (Zhao et al., 1996). However, as the mice reach puberty, many homozygous mutants show substantial recovery of germ cell proliferation. Therefore, it is speculated that, in the absence of BMP8B protein, other BMPs partially rescue the male germ cell deficiency of the *Bmp8b* mutants. BMP8A protein is one of the candidates to fulfill such a compensatory role. In this report, we have shown that, without a functional *Bmp8a* gene, no obvious germ cell deficiency is observed in the majority of the mice during the initiation of spermatogenesis. Two possibilities may account for such a phenotype. The first is that *Bmp8b* is the major player for male germ cell proliferation, while *Bmp8a* has only a minor role, so that loss of *Bmp8a* does not significantly affect early spermatogenesis. The second possibility is that *Bmp8a* transcripts are not translated in early male germ cells during the initiation of spermatogenesis. We favor the first hypothesis based on the RT-PCR data showing that, during early puberty, the expression levels of *Bmp8a* in testis are significantly lower than those of *Bmp8b* (Fig. 8). Two genetic approaches will also help to distinguish between these two hypotheses. The first is to create mice in which both *Bmp8a* and *Bmp8b* genes are inactivated. If a more severe germ cell deficiency is observed in the double mutants than in *Bmp8b* homozygous mutants, a role for *Bmp8a* in the initiation of spermatogenesis will be uncovered. The second approach is to overexpress BMP8A protein in male germ cells of *Bmp8b* homozygous mutants. A genetic rescue of the *Bmp8b* homozygous mutant phenotype will suggest a role for *Bmp8a* during the initiation of spermatogenesis. Experiments are in progress to address these possibilities.

Bmp8a plays a role in the maintenance of spermatogenesis

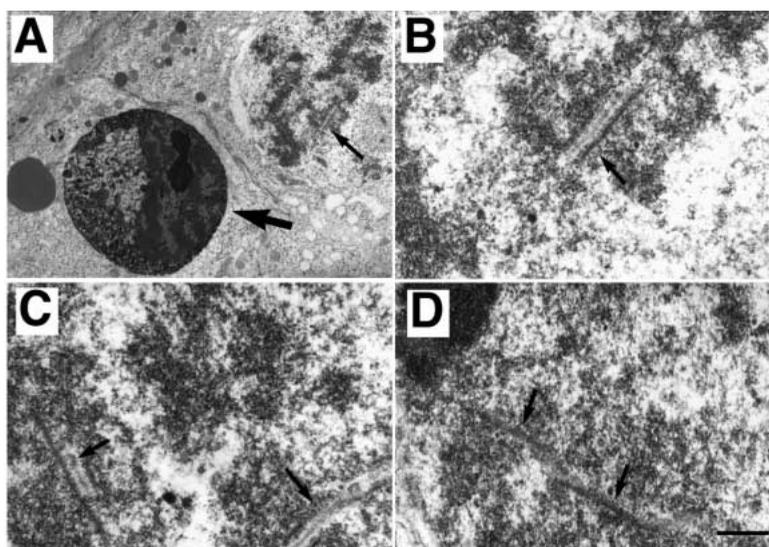After mid-puberty (3.5 weeks of age) and during adult life,

Fig. 7. Ultrastructure of *Bmp8a* mutant testes. Sections were examined under EM and representative areas were photographed. (A) Photograph showing an apoptotic germ cell with darkly stained nucleus (large arrow) adjacent to a relatively normal pachytene spermatocyte with a visible synaptonemal complex (SC) (small arrow). (B) High magnification of A showing SC (small arrow). (C,D) Examples of SC formation in pachytene spermatocytes in two other mutant testes (small arrows). Bar = 2 μm (A), 0.4 μm (B-D).

A

```
Bmp8a 417 GTGGAACGCGACCGTACCCTGGGCTACCAGGAGCCACACTGGAAGGAATTCCACTTTGAC 476
          | | | | | | | | | | | | | | | | | | | | | | | | | | | | | | | | | | | | | | | | | | | | | | | | | | | | | | | | | | | | |
Bmp8b 511 GTGGAACGCGACCGTACCCTGGGCTACCAGGAGCCACACTGGAAGGAATTCCACTTTGAC 570

      477 CTAACCCAGATCCCTGCTGGGGAGGCTGTCACAGCTGCTGAGTTCCGGATCTACAAAGAA 536
          | | | | | | | | | | | | | | | | | | | | | | | | | | | | | | | | | | | | | | | | | | | | | | | | | | | | | | | | | | | | |
      571 CTAACCCAGATCCCTGCTGGGGAGGCTGTCACAGCTGCTGAGTTCCGGATCTACAAAGAA 630

      537 CCCAGCACCCACCCGCTCAACACAACCCTCCACATCAGCATGTTCGAAGTGGTCCAAGAG 596
          | | | | | |   | | | | | | | | | | | | | | | | | | | | | | | | | | | | | | | | | | | | | | | | | | | | | | | | | | | |
      631 CCCAGTACCCACCCGCTCAACACAACCTTCCACATCAGCATGTTCGAAGTGGTCCAAGAG 690

      597 CACTCCAACAGGGAGTCTGACTTGTTCTTTTTGGATCTTCAGACGCTCCGATCTGGGGAC 656
          | | | | | | | | | | | | | | | | | | | | | | | | |   | | | | | | | | | | | | | | | | | | | | | | | | | | | | | | | | |
      691 CACTCCAACAGGGAGTCTGACTTGTCCTTTTTGGATCTTCAGACGCTCCGATCTGGGGAC 750

      657 GAGGGCTGGCTGGTGCTGGACATCACAGCAGCCAGTGACCGATGGCTGCTGAACCATCAC 716
          | | | | | | | | | | | | | | | | | | | | | | | | | | | | | | | | | | | | | | | | | | | | | | | | | | | | | | | | | | | | |
      751 GAGGGCTGGCTGGTGCTGGACATCACAGCAGCCAGTGACCGATGGCTGCTGAACCATCAC 810
                                                                    BamHI
      717 AAGGACCTGGGACTCCGCCTCTATGTGGAAACCGCGGATGGGCACAGCATGGATCCTGGC 776
          | | | | | | | | | | | | | | | | | | | | | | | | | | | | | | | | | | |   | | | | | | | | | | | | |     | | | |   | | | | | | | | | |
      811 AAGGACCTAGGACTCCGCCTCTATGTGGAAACCGAGGATGGGCACGGCATAGATCCTGGC 870

      777 CTGGCTGGTCTGCTTGGACGACAAGCACCACGCTCCAGACAGCCTTTCATGGT 829
          | |   | | | | | | | | | | | | | | | | | | | | | | | | | | | | | | | | | | | | | | | | | | | | | | | |
      871 CTAGCTGGTCTGCTTGGACGACAAGCACCACGCTCCAGACAGCCTTTCATGGT 923
```

Fig. 8. Comparison of *Bmp8a* and *Bmp8b* expression in postnatal testes. (A) Nucleotide sequences of the *Bmp8a* and *Bmp8b* cDNA fragments amplified by RT-PCR with sequences corresponding to primers and *Bam*HI site underlined. Note the base change in *Bmp8b* (bold A) abolishes the *Bam*HI site. The DNA probe used for Southern blot hybridization was from *Bmp8a* (nucleotides 454-771; same as for Fig. 1C). (B) Southern blot hybridization of the *Bam*HI-digested RT-PCR products of *Bmp8a* and *Bmp8b* cDNAs obtained from testis RNA samples of 1-, 2-, 4- and 10-week-old mice. C is the control sample (from 10 week testes) without AMV reverse transcriptase. The *Bmp8a*-specific product is cleaved by *Bam*HI (352 bp), while *Bmp8b* product is unaffected by *Bam*HI (412 bp). Note the greater relative abundance of *Bmp8b* product at earlier stages of postnatal testis development.
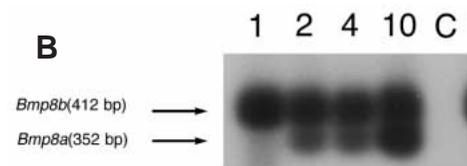
B

Fig. 9. Histological abnormalities of epididymides of homozygous *Bmp8a* mutants and a compound *Bmp8a/Bmp8b* heterozygote. (A) Histology of wild-type adult epididymis showing the efferent duct (ED), initial segment (IS), proximal caput (PC), distal caput (DC), corpus and cauda regions. (B) A section of a cauda epididymis (*Bmp8a−/−*) with advanced granuloma formation in which mature sperm (*) are surrounded by infiltrating leukocytes (arrowhead). (C) A section of a cauda epididymis (*Bmp8a+/−;Bmp8b+/−*) with two foci of granuloma formation outside the epididymis tubule, with sperm (*) in the center and leukocyte infiltration (arrowhead) in the periphery. (D) A section of the same cauda epididymis as in C showing sperm (*) surrounded by infiltrating leukocytes (arrowhead) and the degenerating epididymis tubules. (E) High-power magnification of the boxed region in B showing sperm (*), infiltrating leukocytes (arrowhead) and degenerating tubules (arrow). (F) A high-power magnification of the boxed region in D showing a degenerating epididymis tubule with sperm inside (*). The epithelial layer of the tubule contains multiple vacuoles (arrows), suggesting cell degeneration. (G) A high-power magnification of a section of the same cauda epididymis as in C showing sperm (*) in the neighborhood of an erupted epididymal tubule (arrows). (H) A section through the caput epididymis and testis of a homozygous *Bmp8a* mutant. (I) A higher power magnification of the boxed region in H showing the vacuolated epithelium in the tubules of the distal caput region. (J) A high-power magnification of the boxed region in (I) showing the vacuolated epithelium of the epididymis tubules (arrows). Bar = 800 μm (A-C,H); 200 μm (D,E,I); 50 μm (F,G,J).
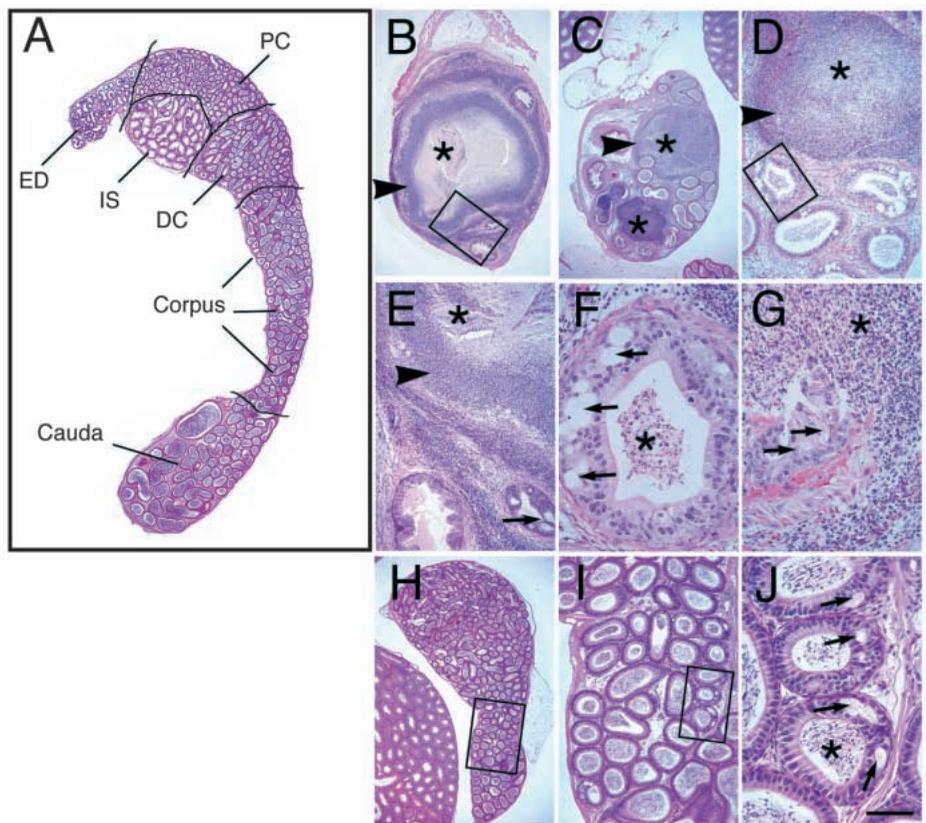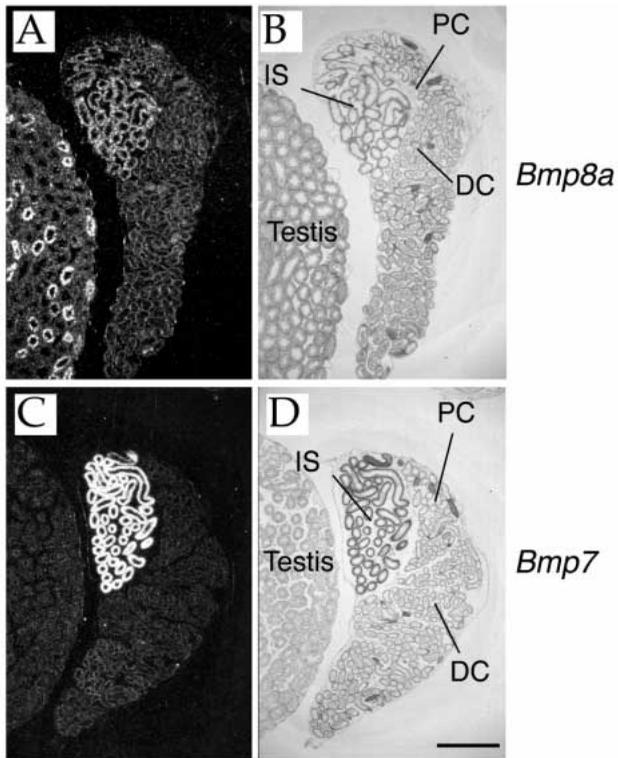
Fig. 10. In situ hybridization showing *Bmp8a* and *Bmp7* expression in the epididymides. (A) A dark-field photomicrograph of a section through a wild-type testis and epididymis hybridized with antisense RNA probe against the 3′ untranslated region of *Bmp8a* mRNA. As reported previously, *Bmp8a* is expressed in the stage 6-8 round spermatids and therefore, shows stage-specific hybridization in the testis. *Bmp8a* transcripts are also detected in the initial segment of the caput epididymis, but at lower levels. (B) A bright-field photomicrograph of A. (C) A dark-field photomicrograph of a section through a wild-type testis and epididymis hybridized with an antisense RNA probe against the pro-region of *Bmp7* mRNA. *Bmp7* transcripts are detected in the initial segment of the caput epididymis at high levels. (D) Corresponding bright-field photomicrograph of C. IS, initial segment; PC, proximal caput; and DC, distal caput. Bar = 800 μm.

specific expression of both *Bmp8a* and *Bmp8b* is maintained in stage 6-8 round spermatids. As reported previously (Zhao et al., 1996), in the absence of a functional *Bmp8b* gene, progressive male germ cell apoptosis results in testis degeneration and sterility of adult animals. Primary spermatocytes are the first cell population to be affected. These cells also express high levels of *Smad1* (Zhao and Hogan, 1997) which encodes a protein acting downstream of BMP receptors and a probable component of the signaling cascade (Sekelsky et al., 1995; Hoodless et al., 1996; Savage et al., 1996; Liu et al., 1996; Massagué, 1996). Therefore, our current model for *Bmp8b* function during the maintenance of spermatogenesis is that BMP8B proteins produced by stage 6-8 round spermatids act on primary spermatocytes to regulate their survival and differentiation.

Although *Bmp8b* is required for the maintenance of spermatogenesis, two important biological questions remain to be addressed. First, in the *Bmp8b* homozygous mutants, the delay in the initiation of spermatogenesis and the reduced

production of differentiated spermatids may contribute to the eventual failure in the maintenance of spermatogenesis. Therefore, the exact role of the stage-specific expression of *Bmp8b* in stage 6-8 round spermatids remains unsolved. This question can be eventually addressed by stage-specific inactivation of *Bmp8b* only in round spermatids. Another related question is the role of *Bmp8a* in stage 6-8 round spermatids. As shown in Fig. 2, there is no obvious difference between the average weights of the wild-type and *Bmp8a* homozygous mutant testes from 1 week up to 12 weeks of age. As the mice age, the testis weight of some mutant animals decreases. Histologically, about 47% of the *Bmp8a* homozygous mutants show different degrees of germ cell degeneration, predominantly through apoptosis, while no overt histological abnormalities were identified in the remaining mutants. Therefore, *Bmp8a* appears to play a role in the maintenance of spermatogenesis. However, further studies are needed to determine which of the two *Bmp8* genes is more important for the maintenance of spermatogenesis.

Evidence that BMPs play a role in maintaining the integrity of the epididymis

The role of BMPs during the development, differentiation and maintenance of the epididymis has not previously been addressed. In this report, we show for the first time that two *Bmps* (*Bmp7* and *8a*) are expressed in the epididymis, specifically in the initial segment of the caput epididymis. Moreover, the inactivation of *Bmp8a* results in a low frequency of degeneration of the epididymis and subsequent granuloma formation and sterility in the mating males. Since BMP8A and BMP7 belong to the same 60A subfamily (Hogan, 1996), it is very likely that they play similar roles and that the absence of BMP8A is compensated by the higher levels of *Bmp7* expression. Furthermore, the fact that major epididymal defects and granuloma formation were only observed in the mating group, but not in the non-mating group, suggests that mating exacerbates the *Bmp8* mutant phenotype in the epididymis. The fact that epididymis degeneration and granuloma formation were also observed in one mating *Bmp8a/Bmp8b* compound heterozygote (Fig. 9C) but not in the mating single heterozygotes suggests that testis-derived BMP8B proteins also play a role in the maintenance of epididymal function.

Our data also reveal that, although *Bmp8a* and *Bmp7* are transcribed in the initial segment of the caput epididymis, the defects observed in *Bmp8a* homozygous mutants are in the distal caput and the cauda regions of the epididymis. This suggests that either BMP8A protein or another growth factor produced locally in response to BMP8A is secreted by the initial segment of the caput and acts as a paracrine molecule on the epithelium of the distal caput and the cauda region of the epididymis to maintain its survival. The fact that two BMP receptors – type I (Suzuki et al., 1994; Mishina et al., 1995) and type II (Kawabata et al., 1995) – and one downstream signaling molecule (SMAD1) are ubiquitously expressed throughout the epithelium of the epididymis (data not shown) does not allow us to distinguish between these possibilities at present.

REFERENCES

Davisson, M. T. (1995). Genetic nomenclature guide (mouse). In *Trends in Genetics Nomenclature Guide* (ed. A. Stewart), pp. 35-38. Kidlington, Oxford, UK: Elsevier Trends Journals.

Dix, D. J., Allen, J. W., Collins, B. W., Mori, C., Nakamura, N., Poorman-Allen, P., Goulding, E. H. and Eddy, E. M. (1996). Targeted gene disruption of Hsp70-2 results in failed meiosis, germ cell apoptosis, and male infertility. *Proc. Natl. Acad. Sci. USA*. **93**, 3264-3268.

Dudley, A. T., Lyons, K. M. and Robertson, E. J. (1995). A requirement for bone morphogenetic protein-7 during development of the mammalian kidney and eye. *Genes Dev.* **9**, 2795-2807.

Furuchi, T., Masuko, K., Nishimune, Y., Obinata, M. and Matsui, Y. (1996). Inhibition of testicular germ cell apoptosis and differentiation in mice misexpressing Bcl-2 in spermatogonia. *Development* **122**, 1703-1709.

Gavrieli, Y., Sherman, Y. and Ben-Sasson, S. A. (1992). Identification of programmed cell death in situ via specific labeling of nuclear DNA fragmentation. *J. Cell. Biol.* **119**, 493-501.

Gelbart, W. M. (1989). The decapentaplegic gene: a TGF-β homologue controlling pattern formation in Drosophila. *Development* **107 Supplement**, 65-74.

Hogan, B. L. M., Blessing, M., Winnier, G. E., Suzuki, N. and Jones, C. M. (1994a). Growth factors in Development: The role of TGF-β related polypeptide signaling molecules in embryogenesis. *Development* **1994 Supplement**, 53-60.

Hogan, B. L. M., Beddington, R. S. P., Costantini, F. and Lacy, E. (1994b). *Manipulating the Mouse Embryo: A Laboratory Manual.* 2nd edition. Plainview, NY: Cold Spring Harbor Laboratory Press.

Hogan, B. L. M. 1996. Bone morphogenetic proteins: multifunctional regulators of vertebrate development. *Genes Dev.* **10**, 1580-1594.

Hoodless, P. A., Haerry, T., Abdollah, S., Stapleton, M., O'Connor, M. B., Attisano, L. and Wrana, J. L. (1996). MADR1, a MAD-related protein that functions in BMP2 signaling pathways. *Cell* **85**, 489-500.

Kawabata, M., Chytil, A. and Moses, H. L. (1995). Cloning of a novel type II serine/threonine kinase receptor through interaction with the type I transforming growth factor-β receptor. *J. Biol. Chem.* **270 (10)**, 5625-5630.

Kingsley, D. M., Bland, A. E., Grubber, J. M., Marker, P. C., Russell, L. B., Copeland, N. G. and Jenkins, N. A. (1992). The mouse short ear skeletal morphogenesis locus is associated with defects in a bone morphogenetic member of the TGF beta superfamily. *Cell* **71**, 399-410.

Kingsley, D. M. (1994). The TGF-β superfamily: new members, new receptors, and new genetic tests of function in different organisms. *Genes Dev.* **8**, 133-146.

Liu, F., Hata, A., Baker, J. C., Doody, J., Carcamo, J., Harland, R. M. and Massagué, J. (1996). A human Mad protein acting as a BMP-regulated transcriptional activator. *Nature* **381**, 620-623.

Luo, G., Hofmann, C., Bronckers, A. L. J. J., Sohocki, M., Bradley, A. and Karsenty, G. (1995). BMP-7 is an inducer of nephrogenesis, and is also required for eye development and skeletal patterning. *Genes Dev.* **9**, 2808-2820.

Massagué, J., Attisano, L. and Wrana, J. L. (1994). The TGF-β family and its composite receptors. *Trends Cell Biol.* **4**, 172-178.

Massagué, J. (1996). TGFβ signaling: receptors, transducers, and Mad proteins. *Cell* **85**, 947-950.

McPherron, A. C. and Lee, S.-J. (1996). The transforming growth factor β superfamily. In *Growth Factors and Cytokines in Health and Disease* (ed. D. LeRoith) Vol.1B, pp. 357-393. Greenwich, CT: JAI press Inc.

Mishina, Y., Susuki, A., Ueno, N. and Behringer, R. R. (1995). Bmpr encodes a type I bone morphogenetic protein receptor that is essential for gastrulation during mouse embryogenesis. *Genes Dev* **9**, 3027-3037.

Özkaynak, E., Schnegelsberg, P. N., Jin, D. F., Clifford, G. M., Warren, F. D., Drier, E. A. and Oppermann, H. (1992). Osteogenic protein-2, a new member of the transforming growth factor-β superfamily expressed early in embryogenesis. *J. Biol. Chem.* **267**, 25220-25227.

Rudnicki, M. A., Braun, T., Hinuma, S. and Jaenisch, R. (1992). Inactivation of MyoD in the mouse leads to up-regulation of the myogenic HLH gene myf-5 and results in apparently normal muscle development. *Cell* **71**, 383-390.

Russell, L. D., Ettlin, R. A., Sinha Hihim, A. P. and Clegg, E. D. (1990). Staging for the laboratory mouse. In *Histological and Histopathological Evaluation of the Testis* (ed. L. D. Russell, R. A. Ettlin, A. P. Sinha Hihim and E. D. Clegg), pp. 119-161. Clearwater, FL: Cache River Press.

Savage, C., Das, P., Finelli, A. L., Townsend, S. R., Sun, C.-Y., Baird, S. E. and Padgett, R. W. (1996). Caenorhabditis elegans genes sma-2, sma-3, and sma-4 define a conserved family of transforming growth factor β. *Proc. Natl. Acad. Sci. USA* **93**, 790-794.

Sekelsky, J. J., Newfeld, S. J., Raftery, L. A., Chartoff, E. H. and Gelbart, W. M. (1995). Genetic characterization and cloning of mothers against dpp, a gene required for decapentaplegic function in Drosophila melanogaster. *Genetics* **139**, 1347-1358.

Suzuki, A., Thies, R. S., Yamaji, N., Song, J. J., Wozney, J. M., Murakami, K. and Ueno, N. (1994). A truncated bone morphogenetic protein receptor affects dorsal-ventral patterning in the Xenopus embryo. *Proc. Natl. Acad. Sci. USA* **91**, 10255-10259.

Winnier, G., Blessing, M., Labosky, P. A. and Hogan, B. L. M (1995). Bone morphogenetic protein-4 is required for mesoderm formation and patterning in the mouse. *Genes Dev.* **9**, 2105-2116.

Yagi, T., Ikawa, Y., Yoshida, K., Shigetani, Y., Takeda, N., Mabuchi, I., Yamamoto, T. and Aizawa, S. (1990). Homologous recombination at c-fyn locus of mouse embryonic stem cell with use of diphtheria toxin A-fragment gene in negative selection. *Proc. Natl. Acad. Sci. USA* **87**, 9918-9922.

Zhao, G.-Q. and Hogan, B. L. M. (1996). Evidence that mouse *Bmp8a* (Op2) and *Bmp8b* are duplicated genes that play a role in spermatogenesis and placental development. *Mech. Dev.* **57**, 159-168.

Zhao, G.-Q., Deng, K., Labosky, P. A., Liaw, L. and Hogan, B. L. M. (1996). The gene encoding bone morphogenetic protein 8B (BMP8B) is required for the initiation and maintenance of spermatogenesis in the mouse. *Genes Dev.* **10**, 1657-1669.

Zhao, G.-Q. and Hogan, B. L. M. (1997). Evidence that Mothers-against-dpp-related 1 (Madr1) plays a role in the initiation and maintenance of spermatogenesis in the mouse. *Mech. Dev.* **61**, 63-73.